INRIA

INSTITUT NATIONAL DE RECHERCHE EN INFORMATIQUE ET EN AUTOMATIQUE

Analysis of hybrid RD-Galerkin schemes for Navier-Stokes simulations

Jiří Dobeš — Mario Ricchiuto — Remi Abgrall — Herman Deconinck

N° 7220

January 2010

Thème NUM

Rapport de recherche

ISSN 0249-6399 ISRN INRIA/RR--7220--FR+ENG

INSTITUT NATIONAL
DE RECHERCHE
EN INFORMATIQUE
ET EN AUTOMATIQUE

INRIA

centre de recherche
BORDEAUX - SUD OUEST

Analysis of hybrid RD-Galerkin schemes for Navier-Stokes simulations

Jiří Dobeš*, Mario Ricchiuto†, Remi Abgrall‡, Herman Deconinck§

Thème NUM — Systèmes numériques
Équipes-Projets BACCHUS

Rapport de recherche n° 7220 — January 2010 — 27 pages

Abstract: We present an extension of multidimensional upwind residual distribution schemes to viscous flows. Following [Ricchiuto *et al. J.Comp.Appl.Math.*, 2007], we consider the consistent coupling of a residual distribution (RD) discretization of the advection operator with a Galerkin approximation for the second order derivatives. Consistency is intended in the sense of uniform accuracy with respect to variations of the mesh size or, equivalently, for the advection diffusion equation, of the Peclet number. Starting from the scalar formulation given in [Ricchiuto *et al. J.Comp.Appl.Math.*, 2007], we perform an accuracy and stability analysis to justify and extend the approach to the time-dependent case. The theoretical predictions are cofirmed by numerical grid convergence studies. The schemes are formally extended to the system of laminar Navier-Stokes equations, and compared to more classical finite volume discretizations on the solution of standard test problems.

Key-words: numerical analysis, second order schemes, parabolic problems, residual distribution, uniform accuracy, unstructured grids

* Boston Consulting Group
† INRIA - Bordeaux Sud-Ouest
‡ INRIA - Bordeaux Sud-Ouest
§ von Karman Institute

Centre de recherche INRIA Bordeaux – Sud Ouest
Domaine Universitaire - 351, cours de la Libération 33405 Talence Cedex
Téléphone : +33 5 40 00 69 00

Analysis of hybrid RD-Galerkin schemes for Navier-Stokes simulations

Résumé : We present an extension of multidimensional upwind residual distribution schemes to viscous flows. Following [Ricchiuto *et al. J.Comp.Appl.Math.*, 2007], we consider the consistent coupling of a residual distribution (RD) discretization of the advection operator with a Galerkin approximation for the second order derivatives. Consistency is intended in the sense of uniform accuracy with respect to variations of the mesh size or, equivalently, for the advection diffusion equation, of the Peclet number. Starting from the scalar formulation given in [Ricchiuto *et al. J.Comp.Appl.Math.*, 2007], we perform an accuracy and stability analysis to justify and extend the approach to the time-dependent case. The theoretical predictions are cofirmed by numerical grid convergence studies. The schemes are formally extended to the system of laminar Navier-Stokes equations, and compared to more classical finite volume discretizations on the solution of standard test problems.

Mots-clés : numerical analysis, second order schemes, parabolic problems, residual distribution, uniform accuracy, unstructured grids

Contents

1 Introduction

In this work we focus on the development of second order discretizations for the simulation of compressible laminar flows. To analyze different approaches, we will study the simple model given by the advection-diffusion equation

$$u_t + \vec{\lambda} \cdot \nabla u = \nabla \cdot (\nu \nabla u) \tag{1}$$

in d spatial dimensions. We will focus to the case of $d = 2$.

In particular, let us start by considering the approximation of solutions to the steady limit of (1). Suppose we are given a triangulation of the two-dimensional spatial domain, and denote by E the generic element of the mesh. In this paper, we will consider methods that can be put in the form

$$u_i^{n+1} = u_i^n - \alpha_i \sum_{E|\, i \in E} \varphi_i^E, \tag{2}$$

where, (at least) for $\nu = 0$

$$\sum_{j \in E} \varphi_j^E = \int_E \lambda \cdot \nabla u_h^n \, dx = \varphi^E \tag{3}$$

with u_h^n the piecewise linear continuous interpolation of the values of the unknown in the nodes of the grid at iteration n, denoted by u_i^n, and with $\alpha_i > 0$

a relaxation parameter. With φ_i^E we denote the contribution to the equation for node i coming from the element E. In particular, for pure advection, these local residuals can be seen as fractions of the element residual φ^E, defined by (3). In this case the schemes reduce to the well known Residual Distribution (RD) of Fluctuation Splitting (FS) schemes [10]

When diffusion is present, the approach often used in practice is to add to an upwind distribution of the residual (3) a Galerkin approximation of the diffusion operator [16, 10]. Several applications of this hybrid discretization are shown in [15].

As remarked in [9], and later in [12], this approach is not satisfactory because it ultimately leads to a loss of accuracy. In particular, even though on coarse meshes second order might be obtained in practice, the accuracy reduces to first order as on refines the grid. The objective of this paper, is to study the approach proposed in [11, 12], where the residual discretizations of the viscous problem is written as the perturbation of the Galerkin discretization

$$\varphi_i^E = \varphi_i^{\mathrm{a,G}} + \varphi_i^{\mathrm{d,G}} + \xi(\varphi_i^{\mathrm{a,RD}} - \varphi_i^{\mathrm{a,G}}), \tag{4}$$

where $\varphi_i^{\mathrm{a,RD}}$ stands for the contribution from the residual discretization of advective terms, $\varphi_i^{\mathrm{a,G}}$ stands for the Galerkin discretization of advective terms and $\varphi_i^{\mathrm{d,G}}$ stands for the Galerkin discretization of the diffusive terms. The local switch $\xi \in [0, 1]$ depends on the cell Peclet (or cell Reynolds) number as

$$\xi(Pe^E) = \begin{cases} 0 & \text{for} \quad Pe^E \to 0 \\ 1 & \text{for} \quad Pe^E \to \infty \end{cases} \tag{5}$$

with *e.g.*

$$Pe^E = \frac{\|\lambda\| h}{\nu} \tag{6}$$

where h the characteristic size of element E. In the following text, we drop all the superscripts E, whenever the reference to the local element is clear from the context.

Provided that second order RD discretization is used, this formulation gives stable and second order accurate solution for limiting cases $Pe \to 0$ and $Pe \to \infty$. In the first case, the discretization boils to the central scheme, which is positive (under certain conditions) for the diffusion problem. In the later case $Pe \to \infty$ it gives the standard second order RD scheme.

2 Numerical schemes for steady problems

2.1 Scalar equation. Solution I

First, we focus on the LDA scheme, with the nodal contribution given as

$$\varphi_i^{\mathrm{a,LDA}} = \beta_i^{\mathrm{LDA}} \varphi^E, \qquad \beta_i^{\mathrm{LDA}} = \frac{k_i^+}{\sum_{j \in E} k_j^+} \tag{7}$$

with element residual

$$\varphi^{\mathrm{a},E} = \sum_{j \in E} k_j u_j. \tag{8}$$

Here k_j is the upwind parameter defined as

$$k_j = \frac{\vec{\lambda} \cdot \vec{n}_j}{d}, \tag{9}$$

where $\vec{n}_j$ is the normal perpendicular to the face opposite of node j scaled by its surface and d is the number of spatial dimensions. Distribution coefficient for the method (4) can be written as

$$\beta_i^* = [1 - \xi(Pe)]\beta^{\mathrm{Gal}} + \xi(Pe)\beta_i^{\mathrm{RD}} = \frac{1 - \xi(Pe)}{d+1} + \xi(Pe)\beta_i^{\mathrm{RD}}. \tag{10}$$

The Galerkin scheme for advection problem (for linear advection equation) is obtained by simply taking distribution coefficient $\beta = 1/3$. Galerkin scheme for the diffusion problem is given by

$$\varphi_i^{\mathrm{d,G}} = \nu \sum_{j \in E} \frac{\vec{n}_i \cdot \vec{n}_j}{d^2 \mu(E)} u_j. \tag{11}$$

First question is, how to define the cell Peclet number for a number of spatial dimensions bigger than one, $d > 1$, how to approximate velocity and how to choose characteristic size of the element. The approach in [11] takes

$$Pe = \frac{\|\lambda\|_{L^2} h^{dD}}{\nu}, \qquad h^{2D} = 2\sqrt{\frac{\mu(E)}{\pi}}, \qquad h^{3D} = \sqrt[3]{3\frac{\mu(E)}{4\pi}}, \tag{12}$$

what is chosen such that h recovers the circle or ball diameter in higher dimension. Anther approach is to define the Peclet number on a basis of the ratio of the cell residuals, namely advection and diffusion residual

$$Pe = \frac{\int_E \lambda \cdot \nabla u \,\mathrm{d}x}{\int_E \nu \Delta u_{xx}} \approx \frac{\mu(E)\|\lambda\| \frac{\delta u}{h}}{\mu(E)\nu \frac{\delta u}{h^2}} \approx \frac{\|\lambda\| h}{\nu}, \tag{13}$$

where δu stands for the value proportional to the variation of the solution u over the element. The problem is, that the diffusive element residual

$$\varphi^{\mathrm{d},E} = \sum_{i \in E} \varphi_i^{\mathrm{d}} \tag{14}$$

is always zero for linear elements. Hence some norm of the nodal contributions has to be chosen. The advantage of this approach is, that it is not necessary to determine velocity and the characteristic size element. However, the choice of the norm of the residual is also not unique. Among the possible choices one can select e.g.

$$Pe = \frac{\sum_{i \in E} |\varphi_i^a|}{\sum_{i \in E} |\varphi_i^d|}, \qquad Pe = \sqrt{\frac{\sum_{i \in E} (\varphi_i^a)^2}{\sum_{i \in E} (\varphi_i^d)^2}}. \tag{15}$$

We will use the first option in this work.

The blending coefficient has to be chosen such that

$$\xi(0) = 0, \qquad \xi(\infty) = 1. \tag{16}$$

Actually, *any* scheme written as (4) is second order accurate for $h \to 0$ if it respects $\xi \to 0$ for $Pe \to 0$.[1] One choice is

$$\xi(Pe) = \max(1, Pe). \tag{17}$$

This is a simple choice and it respects our first requirement, i.e. RD method is obtained for $Pe \to \infty$ and Galerkin method for $Pe \to 0$. However, e.g. for 1D problem and $Pe \approx 1$ we get the upwind discretization of advection term with central discretization of the diffusion term, and this discretization has the truncation error of first order.

To have better idea, how the blending coefficient should look like, we will examine advection–diffusion equation in 1D with Euler forward time integration procedure

$$\frac{u_i^{n+1} - u_i^n}{\Delta t} = -\xi \frac{u_i^n - u_{i-1}^n}{\Delta x} - (1-\xi)\frac{u_{i+1}^n - u_{i-1}^n}{2\Delta x} + \nu \frac{u_{i+1}^n - 2u_i^n + u_{i-1}^n}{\Delta x^2} \tag{18}$$

with $a > 0$ and we will find a lower bound on $\xi(Pe)$ for scheme positivity. We gather terms into the form of

$$u_i^{n+1} = c_0 u_i^n + c_{+1} u_{i+1}^n + c_{-1} u_{i-1}^n. \tag{19}$$

For the positivity of the scheme, positivity of the coefficients is required $c_0 \geq 0$, $c_1 \geq 0$, $c_{-1} \geq 0$. The first condition gives us a time step restriction

$$\Delta t \leq \frac{1}{\xi \frac{a}{\Delta x} + \frac{\nu}{\Delta x^2}} \tag{20}$$

and the last condition is always satisfied. The second condition gives us restriction for the blending coefficient

$$\xi \geq 1 - \frac{1}{Pe}, \tag{21}$$

what is a lower bound for the positivity of the scheme. Since the central scheme has lower error than the upwind scheme, it is desirable to have ξ as small as possible. We can take

$$\xi(Pe) = \max(0, 1 - \frac{1}{Pe}). \tag{22}$$

In this case, the scheme reduces to the second order, positive Galerkin method for $Pe \leq 1$.

In the case of two spatial dimensions, the Galerkin scheme for the diffusive part of the equation is positive if the triangulation is Delaunay. The positivity criterion for the Galerkin scheme for both advection and diffusion discretization can be found only for very special arrangements of the mesh.

2.2 Scalar equation. Solution II

The other approach is to use fully residual scheme, where the viscous part is included into the residual. The scheme looks like

$$\varphi_i = \beta_i(\varphi^{\mathrm{a}} + \varphi_i^{\mathrm{d}}), \tag{23}$$

[1] As long as $\xi(Pe)$ behaves as a linear function for $Pe \to 0$.

where β_i is the distribution coefficient, φ^{a} is the advection residual and φ_i^{d} is the diffusion residual.

We can compute gradient in nodes, denoted by $(\nabla u)^h$, e.g. by the least square reconstruction from neighboring nodes. The diffusion residual is to be approximated as

$$\varphi_i^{\mathrm{d}} \approx \int_E \nabla[\mu\,(\nabla u)^h]\,\mathrm{d}x. \tag{24}$$

We will evaluate this scheme in one dimension. Nodal gradients (derivatives) are given by the central discretization

$$\left(\frac{\partial u}{\partial x}\right)_i^h \approx \frac{u_{i+1}-u_{i-1}}{2\Delta x}. \tag{25}$$

The fully discrete scheme is

$$\frac{u_i^{n+1}-u_i^n}{\Delta t} + a\frac{u_i^n-u_{i-1}^n}{\Delta x} = \frac{\nu}{\Delta x}\left[\frac{u_{i+1}^n-u_{i-1}^n}{2\Delta x} - \frac{u_i^n-u_{i-2}^n}{2\Delta x}\right]. \tag{26}$$

It can be written as

$$u_i^{n+1} = \frac{\nu\Delta t}{\Delta x^2}u_{i+1}^n + \left(1-\frac{\Delta t a}{\Delta x}-\frac{\nu\Delta t}{\Delta x^2}\right)u_i^n + \left(\frac{\Delta t a}{\Delta x}-\frac{\nu\Delta t}{\Delta x^2}\right)u_{i-1}^n + \frac{\nu\Delta t}{\Delta x^2}u_{i-2}^n. \tag{27}$$

First and last term on the RHS are always positive, the second term is positive under a time step constrain eq. (20). The third term is positive if $Pe > 1$. As a conclusion, this scheme is positive for $Pe > 1$ under a time-step restriction.

In order to resolve problem with positivity, it can be blended with Galerkin scheme for $Pe \to 0$, as in the previous approach. For this scheme we present only the theoretical result, we didn't include any numerical experiments.

2.3 Viscous compressible fluid flow

We present rather straight-forward extension of the method to the system of equations. We use the linearized Galerkin method, which reduces to the central discretization, with distribution matrix

$$\beta_i = \frac{1}{d+1}\mathbf{I}. \tag{28}$$

The Peclet number we define with the accordance with the definition for the scalar problem (15) as

$$Pe = \frac{\sum_{i\in E}\|\varphi_i^a\|_{L_2}}{\sum_{i\in E}\|\varphi_i^d\|_{L_2}}. \tag{29}$$

We can easily modify the distribution coefficients analogously to the eq. (10). In the case, there the distribution matrices are not explicitly defined, and only nodal contribution φ_i are known (and the element residual φ^E as its sum), the following modification can be applied:

$$\varphi_i^* = \xi(Pe)\varphi_i + \frac{1-\xi(Pe)}{d+1}\varphi^E. \tag{30}$$

The discretization of viscous terms is a strait-forward extension of (11), for more discussion see e.g. [16].

2.4 Finite volume scheme

We have used a *cell centered* finite volume scheme for the comparison. The variables are stored in centers of mesh elements. The method uses linear least square reconstruction, with Barth's limiter [1] as a option. The numerical flux is approximated by the Roe's Riemann solver [13] in the case of Navier-Stokes equations, or simple upwind flux in the case of scalar equations. The discretization of viscous fluxes is done on dual grid. Solution from elements centers are interpolated to vertices of the mesh. Derivatives are then approximated on auxiliary volumes connecting centroids of the cell with mesh vertices.

3 Numerical experiments for steady problems

3.1 Steady scalar advection-diffusion equation

First, we repeat test case from [9, 11]. We solve the equation (1) on spatial domain $[0,1]^2$, with $\vec{\lambda} = (\lambda_x, \lambda_y) = (0,1)$, $\nu = 0.01$. The problem has exact solution

$$u = -\cos(2\pi\eta)\exp(\frac{\zeta(1-\sqrt{1+16\pi^2\nu^2})}{2\nu}), \tag{31}$$

with $\eta = \lambda_y x - \lambda_x y$ and $\zeta = \lambda_x x + \lambda_y y$.

We use a sequence of unstructured meshes with $h = 1/10,\ 1/20,\ 1/40,\ 1/80,\ 1/150,\ 1/300$. This corresponds to the cell Peclet numbers of range $Pe = [0.33, 10]$. Results are shown in Fig. 1. One can see that the original scheme deviates from the second order slope for $Pe \lessapprox 3$, where both modifications continue in the second order convergence. The newer modification (22) gives the lower error, as expected.

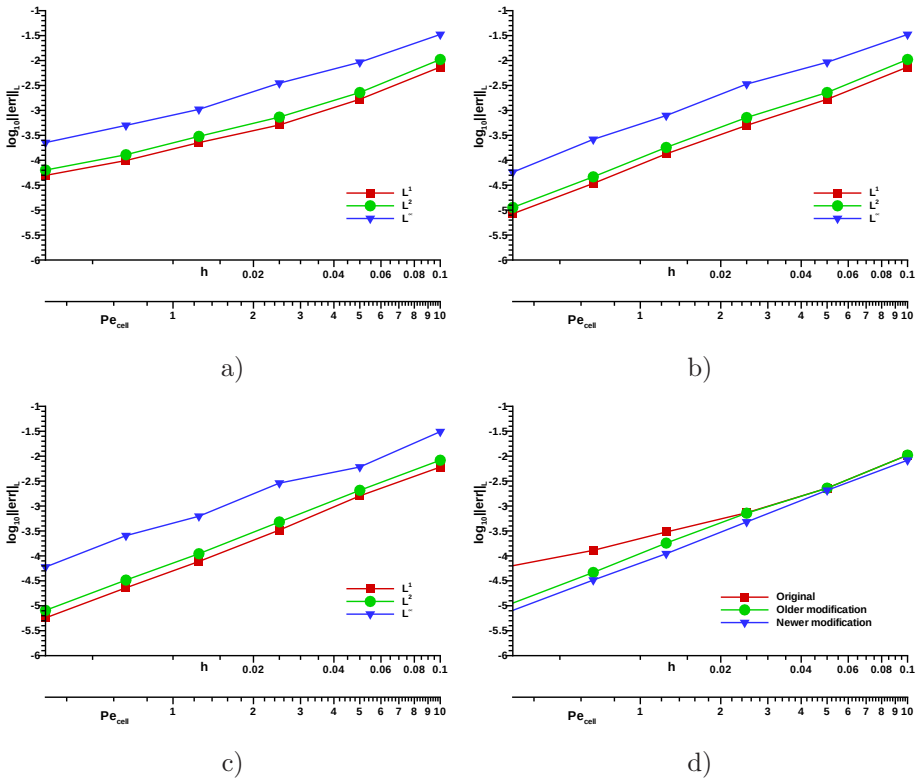

Figure 1: 2D advection-diffusion equation, test eq. (31). a) Original distribution coefficients, i.e. LDA scheme for inviscid terms and Galerkin scheme for viscous terms. b) modification of the distribution coefficients given by eqns. (12), (17) (older modification) c) modification of the distribution coefficients given by eqns. (13), (22) (newer modification). d) comparison of different modifications in L^2 norm.

3.2 Incompressible laminar boundary layer – Blasius's solution

The classical Blasius similarity solution provides data for the comparison. The text by White [18] or Schlichting [14] discusses this solution.

Parameters and mesh size were taken from the web page `http://www.grc.nasa.gov/WWW/wind/valid/fp` The grid points are evenly spaced along the plate. The normal grid points are placed at constant η coordinates, where

$$\eta = \frac{y}{\sqrt{\frac{u_\infty}{2\nu x}}}, \tag{32}$$

with the grid evenly spaced until $\eta = 4$ and then spaced by a factor of 1.1 until the outer boundary at $\eta = 50$ is reached. For $x < 0.3$ the y coordinate is the same as $x = 0.3$. Final grid resolution is 52×35 elements. There are 13 nodes in the x direction prior to leading edge of the flat plate. Fig. 2 shows how the grid looks like.

We compute a flow over the flat plate with a free stream Mach number $Ma = 0.3$ and the Reynolds number based on the length of the flat plate is approx. $2 \cdot 10^5$. We have set the following free stream conditions: $\rho_\infty = 1.4$, $u_\infty = 0.3$, $p_\infty = 1$, $\nu = 1.5 \cdot 10^{-6}$. The self-similar solution gives

$$c_f = \frac{\frac{\partial u}{\partial y}\big|_w}{\sqrt{Re_x}}, \qquad Re_x = \frac{u_e x}{\nu}, \qquad \left.\frac{\partial u}{\partial y}\right|_w = 0.664067. \tag{33}$$

Technically important is a value of c_f coefficient

$$c_f = \frac{\tau_w}{\frac{1}{2}\rho_e u_e^2}, \qquad \tau_w = \nu \left.\frac{\partial u}{\partial y}\right|_{y=0}. \tag{34}$$

The Fig. 3 shows the distribution of the cell Peclet number together with the blending coefficient away from the plate. Figs. 4 to 7 shows the solution in terms of isolines of the Mach number. One can notice that all the solutions are very similar. Distribution of the friction coefficient along the plate is shown in Fig. 8 and the cut of the u velocity in Fig. 9.

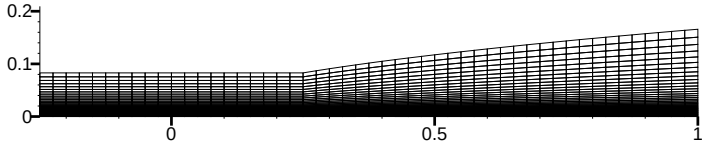

Figure 2: Mesh for laminar incompressible flow over a flat plate

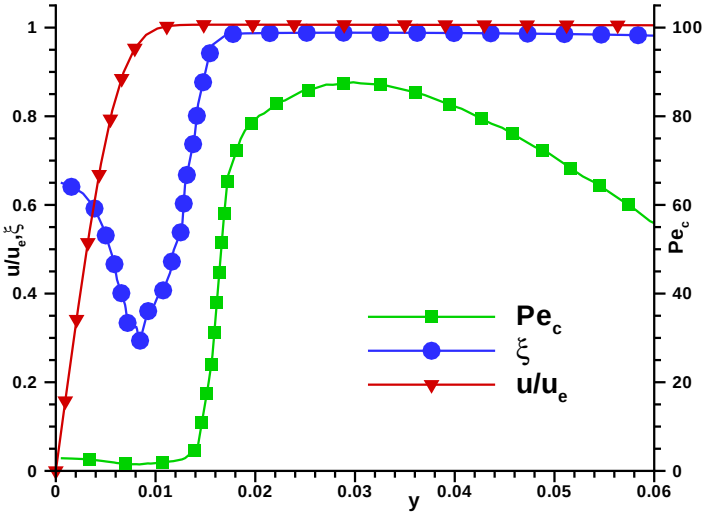

Figure 3: Cell Peclet number at $x = 0.8$, together with the blending coefficient ξ and the distribution of the velocity.

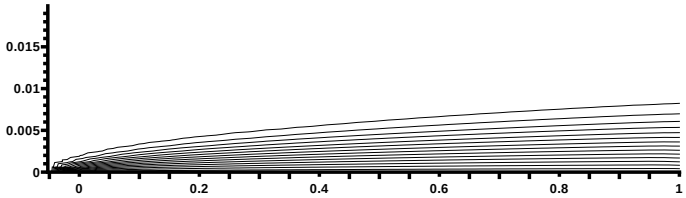

Figure 4: Isolines of Mach number. LDA scheme with the blending coefficient given by (29), (22).

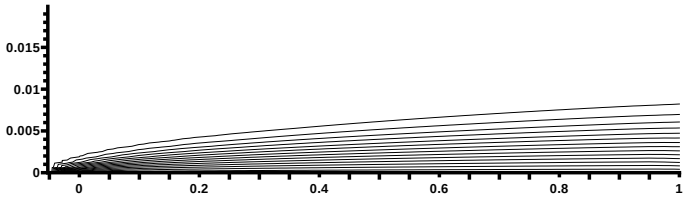

Figure 5: Isolines of Mach number. LDA scheme with $\xi \equiv 1$.

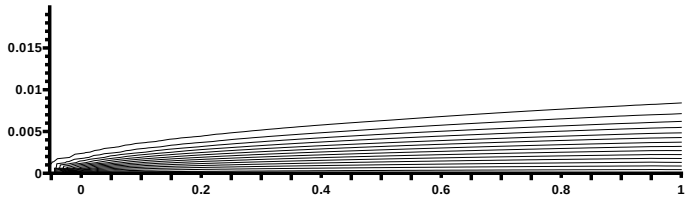

Figure 6: Isolines of Mach number. N-modified scheme with the blending coefficient given by (29), (22)

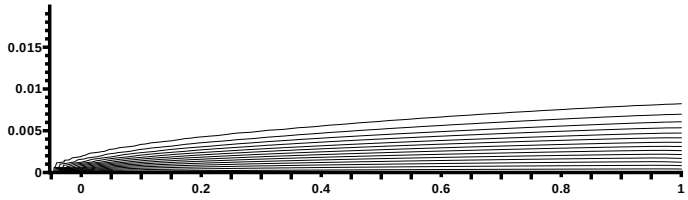

Figure 7: Isolines of Mach number. Bx scheme (see [7]) with the blending coefficient given by (29), (22)

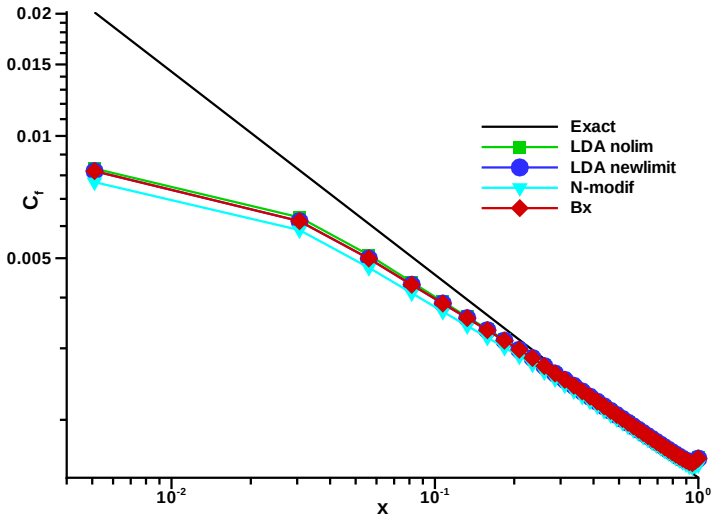

Figure 8: Distribution of the friction coefficient along the plate. RD schemes.

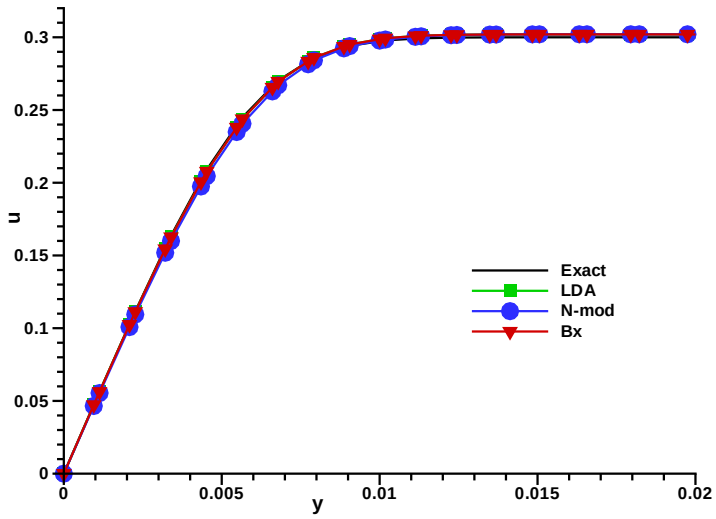

Figure 9: Cut at $x = 0.8$. Distribution of the velocity u. Full line corresponds to the Blasius solution.

3.3 Steady flow past NACA0012: $Ma = 2$, $Re = 106$, $\alpha = 10°$

This test case is taken from [2]. The computational mesh is shown in Figs. 10 and 11, solution with the LDA scheme in Fig. 12. The friction along the airfoil is plotted in Fig. 13. There is virtually no difference in the friction coefficient in the modified version of the RD scheme.

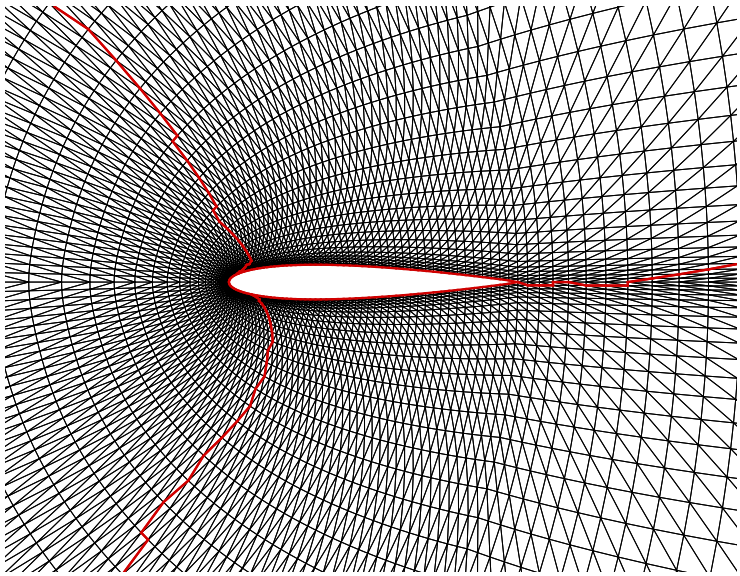

Figure 10: NACA 0012 $Ma = 2$ $Re = 106$, $\alpha = 10°$. Computational mesh.

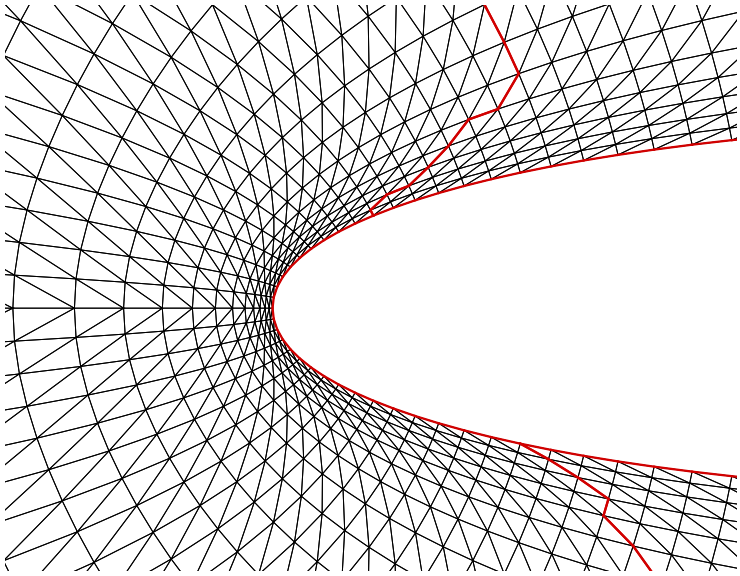

Figure 11: NACA 0012 $Ma = 2$ $Re = 106$, $\alpha = 10°$. Computational mesh – zoom.

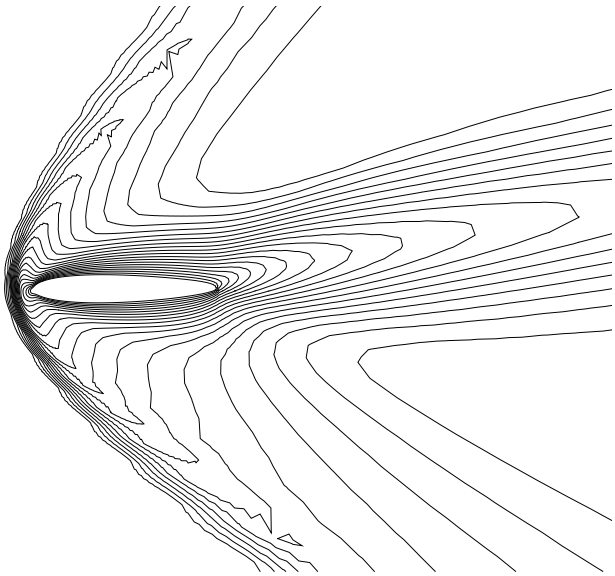

Figure 12: NACA 0012 $Ma = 2$ $Re = 106$, $\alpha = 10°$. Isolines of Mach number.

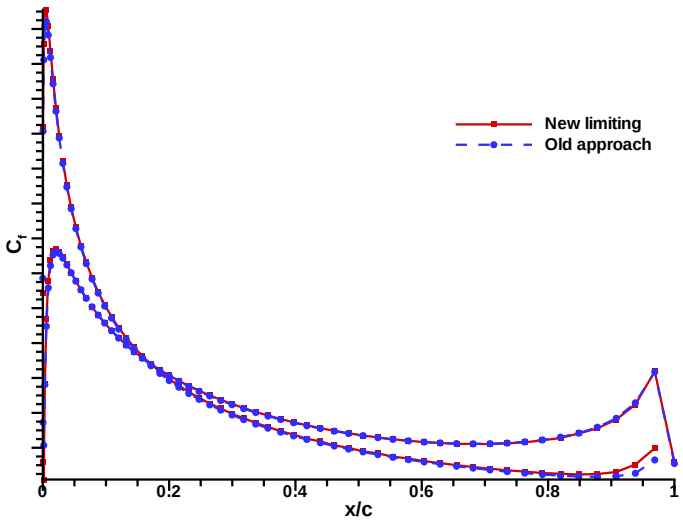

Figure 13: NACA 0012 $Ma = 2$ $Re = 106$, $\alpha = 10°$. (Scaled) friction. Comparison of the LDA scheme with $\xi \equiv 1$ (denoted by old approach) and the blending coefficient given by (29), (22) (denoted as the new limiting).

4 Numerical schemes for time dependent problems

4.1 Scalar equation. Solution I

Now, we will investigate time-dependent problem

$$u_t + \vec{\lambda} \cdot \nabla u = \nu \Delta u. \tag{35}$$

The dual-time (or space-time) nodal contribution is will be taken again as

$$\varphi_i = \varphi_i^{\mathrm{a,G}} + \varphi_i^{\mathrm{d,G}} + \xi(\varphi_i^{\mathrm{a,RD}} - \varphi_i^{\mathrm{a,G}}), \tag{36}$$

where φ_i^{a} include both contributions from the advection terms and time derivative

$$\varphi^{\mathrm{a}} \approx \int_E (u_t + \vec{\lambda} \cdot \nabla u)\, \mathrm{d}\vec{x}. \tag{37}$$

The nodal contribution from the Galerkin scheme including the mass matrix is

$$\varphi_i^{\mathrm{a,G}} = \frac{\mu(E)}{d+1} \sum_{j \in E} \left(\frac{1+\delta_{ij}}{d+2} \frac{\partial u_j}{\partial t} \right) + \frac{1}{d+1} \varphi^E, \tag{38}$$

while for the LDA of Ferrante and Deconinck [8] it is

$$\begin{aligned} \varphi_i^{\mathrm{a,LDA}} = {} & \frac{\mu(E)}{d+1} \left(k_i^+ N + \frac{2}{d+2} I - \frac{1}{d+1} I \right) \frac{\partial u_i}{\partial t} + \\ & + \frac{\mu(E)}{d+1} \sum_{\substack{j \in E \\ j \neq i}} \left[\left(k_j^+ N + \frac{1}{d+2} I - \frac{1}{d+1} I \right) \frac{\partial u_j}{\partial t} \right] + k_i^+ N \varphi^E. \end{aligned} \tag{39}$$

Let us examine the Galerkin scheme first. In 1D, the semi-discrete equation is

$$\frac{1}{6} \frac{\partial u_{i+1}}{\partial t} + \frac{4}{6} \frac{\partial u_i}{\partial t} + \frac{1}{6} \frac{\partial u_{i-1}}{\partial t} + a \frac{u_{i+1} - u_{i-1}}{2\Delta x} = \nu \frac{u_{i+1} + 2u_i - u_{i-1}}{\Delta x^2}. \tag{40}$$

The fully discrete version using the Crank-Nicholson time integration method is then

$$\begin{aligned} \frac{1}{6} \frac{u_{i+1}^{n+1} - u_{i+1}^n}{\Delta t} + \frac{4}{6} \frac{u_i^{n+1} - u_i^n}{\Delta t} + \frac{1}{6} \frac{u_{i-1}^{n+1} - u_{i-1}^n}{\Delta t} + & \\ \frac{1}{2} \left[a \frac{u_{i+1} - u_{i-1}}{2\Delta x} - \nu \frac{u_{i+1} + 2u_i - u_{i-1}}{\Delta x^2} \right]^{n+1} + & \\ \frac{1}{2} \left[a \frac{u_{i+1} - u_{i-1}}{2\Delta x} - \nu \frac{u_{i+1} + 2u_i - u_{i-1}}{\Delta x^2} \right]^{n} = 0. & \end{aligned} \tag{41}$$

The fully discrete version of the LDA scheme with the Crank-Nicholson time integration and central discretization of the viscous terms is

$$\begin{aligned} & \left(\frac{5}{12\Delta t} - \frac{1}{2} \frac{a}{\Delta x} - \frac{1}{2} \frac{\nu}{\Delta x^2} \right) u_{i-1}^{n+1} + \left(\frac{2}{3\Delta t} + \frac{1}{2} \frac{a}{\Delta x} + \frac{\nu}{\Delta x^2} \right) u_i^{n+1} + \left(-\frac{1}{12\Delta t} - \frac{1}{2} \frac{\nu}{\Delta x^2} \right) u_{i+1}^{n+1} + \\ & \left(-\frac{5}{12\Delta t} - \frac{1}{2} \frac{a}{\Delta x} - \frac{1}{2} \frac{\nu}{\Delta x^2} \right) u_{i-1}^{n} + \left(-\frac{2}{3\Delta t} + \frac{1}{2} \frac{a}{\Delta x} + \frac{\nu}{\Delta x^2} \right) u_i^{n} + \left(\frac{1}{12\Delta t} - \frac{1}{2} \frac{\nu}{\Delta x^2} \right) u_{i+1}^{n} \\ & = 0. \end{aligned} \tag{42}$$

Now, we take a blend between the LDA and the Galerkin scheme with the blending coefficient ξ, giving

$$\begin{aligned}\left[\xi\left(\frac{5}{12\Delta t}-\frac{1}{2}\frac{a}{\Delta x}\right)+(1-\xi)\left(\frac{1}{6\Delta t}-\frac{1}{4}\frac{a}{\Delta x}\right)-\frac{1}{2}\frac{\nu}{\Delta x^2}\right]u_{i-1}^{n+1}+\\ \left[\frac{2}{3\Delta t}+\frac{\xi}{2}\frac{a}{\Delta x}+\frac{\nu}{\Delta x^2}\right]u_{i}^{n+1}+\\ \left[\xi\left(-\frac{1}{12\Delta t}\right)+(1-\xi)\left(\frac{1}{6\Delta t}+\frac{1}{4}\frac{a}{\Delta x}\right)-\frac{1}{2}\frac{\nu}{\Delta x^2}\right]u_{i+1}^{n+1}+\\ \left[\xi\left(-\frac{5}{12\Delta t}-\frac{1}{2}\frac{a}{\Delta x}\right)+(1-\xi)\left(-\frac{1}{6\Delta t}-\frac{1}{4}\frac{a}{\Delta x}\right)-\frac{1}{2}\frac{\nu}{\Delta x^2}\right]u_{i-1}^{n}+\\ \left[-\frac{2}{3\Delta t}+\frac{\xi}{2}\frac{a}{\Delta x}+\frac{\nu}{\Delta x^2}\right]u_{i}^{n}+\\ \left[\xi\left(\frac{1}{12\Delta t}\right)+(1-\xi)\left(-\frac{1}{6\Delta t}+\frac{1}{4}\frac{a}{\Delta x}\right)-\frac{1}{2}\frac{\nu}{\Delta x^2}\right]u_{i+1}^{n}=0. \quad (43)\end{aligned}$$

For $x=0$ it is the Galerkin scheme, while for $\xi=1$ it is the LDA scheme with mass matrix and the central viscous discretization.

After following procedure in [17], we get modified equation

$$\begin{aligned}u_t+au_x=\nu u_{xx}+\left(\frac{1}{2}\xi\nu\Delta x-\frac{1}{12}a^3\Delta t^2\right)u_{xxx}+\\ \left(-\xi\frac{1}{24}a\Delta x^3+\frac{1}{4}a^2\nu\Delta t^2-\frac{1}{12}\nu\Delta x^2+\xi^2\frac{1}{4}\nu\Delta x^2\right)u_{xxxx}. \quad (44)\end{aligned}$$

We will focus on the first term. We take a time-step as

$$\Delta t=\frac{\sigma}{\frac{a}{\Delta x}+\frac{\nu}{\Delta x^2}},\qquad 0<\sigma\leq 1,\quad \sigma\approx 1 \quad (45)$$

and we get

$$\frac{1}{2}\xi\nu\Delta x-\frac{1}{12}a^3\Delta t^2=\frac{1}{2}\nu\Delta x\left(\xi-\underbrace{\frac{1}{6}\frac{\sigma^2Pe^3}{1+Pe^2}}_{\alpha}\right)=\frac{1}{2}\nu\Delta x\left(\xi-\alpha\right). \quad (46)$$

Following behavior can be observed:

- Galerkin scheme ($\xi\equiv 0$): α is of $\mathcal{O}(Pe^3)\approx\mathcal{O}(\Delta x^3)$, it means that RHS term (46) is $\mathcal{O}(\Delta x^4)$. In this case for $\Delta x\to 0$, in equation (44) term u_{xxxx} is dominating, the scheme is second order accurate.
- LDA scheme ($\xi\equiv 1$): for $\Delta x\to 0$ the equation (46) behaves as $\nu\Delta x/2$, the scheme is first order accurate.
- Case $\Delta x \gtrapprox \nu/a$ (i.e. $Pe\gtrapprox 1$): We will check when $\alpha\approx\xi$, i.e. when u_{xxx} truncation error of Galerkin scheme will be the same order as the truncation error of the LDA inviscid + Galerkin viscous scheme. After solving the nonlinear equation, we get $Pe\approx 7.66$. For this particular value of the Peclet number the u_{xxx} the two terms substract and the

truncation error is zero, it might not true in more spatial dimensions. For $Pe \gtrapprox 7.66$ the truncation error coming from the central discretization is of the same order as the truncation error coming from the mismatch of the central discretization of the viscous terms and the upwind discretization of the advection term. On another words, for $Pe > 7.66$ the idea of error reduction with blending of Galerkin and upwind schemes for advection terms does not make much sense anymore, it is good enough to use the upwind scheme for the advection terms and Galerkin scheme for diffusion terms.

Let us check, what is the condition on ξ for the positivity of the scheme (43). The stability analysis of the LDA scheme gives us a time step restriction

$$\Delta t \leq \frac{1}{\frac{a}{2\Delta x} + \frac{\nu}{\Delta x^2}}, \tag{47}$$

or equivalently

$$\gamma = \frac{a\Delta t}{\Delta x} \leq \frac{1}{\frac{1}{2} + \frac{1}{Pe}}. \tag{48}$$

After some algebra, one can conclude that the bound on ξ (if the maximal time-step $\gamma = 1$ is used) is

$$\xi \geq \max\left(0, \frac{Pe-1}{Pe+1}\right). \tag{49}$$

This restriction is actually more relaxed than the one given by the (22). In the following computations, we will still use the value given by (22).

4.2 Viscous compressible fluid flow

We apply the same extension as before.

5 Numerical experiments time dependent problems

5.1 Scalar rotational advection–diffusion problem

We consider an advection-diffusion equation (1) with $\vec{\lambda} = (\lambda_x, \lambda_y) = (-y, x)$, i.e. case of rotation-diffusion, with rotation around origin $(0, 0)$ by angular velocity $\omega = 1$. The solution of a pure diffusion problem rotated with angular velocity ω is the solution of the problem. We first look at the problem

$$u_t = \nu \Delta u \tag{50}$$

in cylindrical coordinates. The problem reads

$$u_t = \nu \left(u_{rr} + \frac{1}{r} u_r + \frac{1}{r^2} u_{\theta\theta} \right). \tag{51}$$

We will look only to radial-symmetric solution, hence last term drops. We will search for the solution using Fourier method, i.e. the solution is in form

$$u(t, r) = T(t)\, R(r). \tag{52}$$

This gives us

$$\frac{T'}{T} = \nu \left(\frac{R''}{R} + \frac{1}{r}\frac{R'}{R} \right) = c_1 \tag{53}$$

The solution of the equation $T'/T = c_1$ is simply $T(t) = c_2 \exp(c_1 t)$. The second equation can be written as

$$r^2 R'' + rR' - r^2 R\frac{c_1}{\nu} = 0 \tag{54}$$

with well known solution in form

$$R(r) = c_3 \mathrm{J}_0(\sqrt{-\frac{c_1}{\nu}}\, r) + c_4 \mathrm{Y}_0(\sqrt{-\frac{c_1}{\nu}}\, r), \tag{55}$$

where J_0 and Y_0 are the Bessel functions of the first and the second kind. Since Y_0 is singular at the $r = 0$, we will not consider this part of the solution. The problem has the solution

$$u(r,t) = c_0 \exp(c_1 t)\, \mathrm{J}_0(\sqrt{-\frac{c_1}{\nu}}\, r). \tag{56}$$

Now, we will turn out attention to the solution of the problem (1)

$$u_t + (-y, x) \cdot \nabla u = \nu \Delta u. \tag{57}$$

The solution is given by the equation (56) with rotated frame of reference. Now, we have to choose the parameters. First, maximal value of the solution after one rotation at the time $t = 2\pi$ is chosen 0.2, starting with $u_0 = 1$. Hence,

$$\exp(2\pi c_1) = 0.2 \tag{58}$$

giving $c_1 = \ln(0.2)/2/\pi$. From the condition $u_0|_{\max} = 1$ the $c_0 = 1$. Now, the viscosity has to be chosen. We set $\nu = 0.005$. The implementation is easy, because the Bessel function is part of the standard C library in the same manner as e.g. `sin()` and it is called `double j0(double x)`.

Finally, the solution is given by

$$u = \exp(c_1 t)\, \mathrm{J}_0(r\sqrt{-\frac{c_1}{\mu}}) \tag{59}$$

with

$$c_1 = \frac{\ln 0.2}{2\pi} \tag{60}$$

$$\alpha = -t \tag{61}$$

$$\tilde{x} = x\cos\alpha - y\sin\alpha + 0.5 \tag{62}$$

$$\tilde{y} = x\sin\alpha + y\cos\alpha \tag{63}$$

$$r = \sqrt{\tilde{x}^2 + \tilde{y}^2}. \tag{64}$$

Initial conditions are plotted in Fig. 14.

The problem was solved with the LDA scheme with original approach, i.e. LDA+Galerkin viscous terms, the Galerkin discretization for all the terms and finally, with above described hybrid approach.

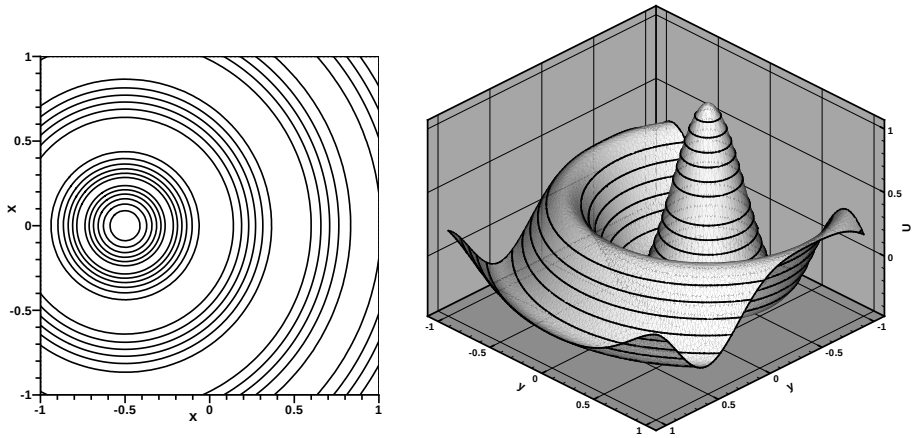

Figure 14: Unsteady rotation-diffusion problem – initial conditions.

Scheme	L^1 order	L^2 order	L^∞ order
LDA inviscid + Galerkin viscous	1.03	1.00	1.00
Galerkin all (unstable for large Pe)	1.96	1.96	1.77
LDA+Galerkin hybrid scheme	2.21	2.23	1.93

Table 1: Comparison of orders of accuracy for 2D unsteady advection-diffusion problem

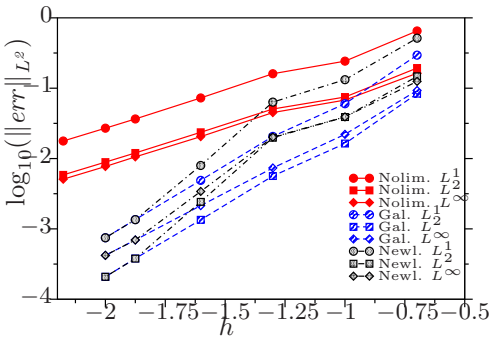

Figure 15: Unsteady rotation-diffusion problem – LDA scheme with mass matrix, convergence study. Nolim.: original version LDA scheme with Galerkin treatment of viscous terms. Gal.: Galerkin central scheme both for advection and diffusion. Newl.: the novel approach, hybrid blending both formulations.

5.2 Flow past suddenly accelerated wall – Rayleigh problem

We solve the problem on domain $\Omega = [0,1] \times [0,1]$. Top-free stream, bottom wall, sides periodic boundary condition. Free stream parameters: $(\rho, u, v, p)_\infty = (1.4, 1, 0, 100)$. Kinematic viscosity is chosen $\nu = 0.1$. We solve the problem for time interval $t \in [0, 0.1]$. The solution is

$$u = u_\infty \mathrm{erf}(\frac{y}{2\sqrt{\nu t}}). \tag{65}$$

The same test case (on finer mesh) was already used in [6, 3, 5, 4].

We use a very coarse mesh with spacing $h = 1/10$ (217 nodes and 392 elements only). Two periods of the solution for the viscous hybrid scheme together with the mesh is plotted in Fig. 16. Unfortunately, there is no visual advantage of the hybrid scheme. Notice much worse performance of the FV scheme with comparison to the RD schemes.

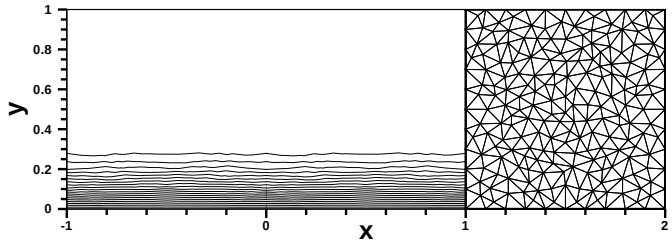

Figure 16: Rayleigh problem. Solution using the LDA scheme with the mass matrix and with viscous hybrid method. Solution at time $t = 0.1$. Two periods plotted together with the computational mesh.

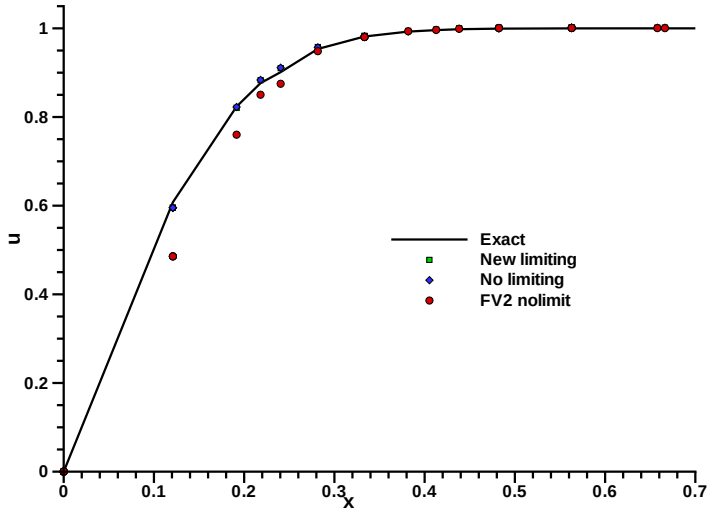

Figure 17: Rayleigh problem. Cut in the y direction for the LDA scheme with hybrid method and with standard method. The finite volume scheme with linear reconstruction is included.

5.3 Vortex shedding past a circular cylinder

Mach number $Ma = 0.1$, Reynolds number $Re = 100$. The laminar vortex shedding starts from $Re \approx 70$, for $Re \leq 70$ the solution is steady. 48 elements is placed around the cylinder. Computations by LDA scheme with and without the new approach was started from already periodic state, precomputed earlier.

The solution is plotted in Fig. 18. There are minor differences between the numerical schemes, even that the cell Reynolds number near the wall is of order 2.

5.4 Transonic vortex pairing

This test case involves a transonic vortex pairing in a mixing layer [19]. The problem consists of a shear layer defined by two free streams with velocity profiles $u = \tanh(2y)/2$, $v = 0$. To these velocity profiles we superimpose the velocity perturbations

$$v' = \sum_{k=1}^{2} a_k \cos(2\pi k x/L_x + \phi_k) \exp(-y^2/b) \tag{66}$$

with parameters $a_1 = 0.01$, $a_2 = 0.05$, $\phi_1 = \phi_2 = \pi/2$, $b = 10$. The u' perturbation is computed from condition $\nabla(u', v') = 0$. The problem has been solved inside a rectangular area $L_x \times L_y$ with $L_x = 30$ and $L_y = 100$. The top and bottom boundaries are treated as inviscid walls, and periodic boundary conditions are set on the left and right boundaries. The kinematic viscosity in the free streams is set to $\nu_\infty = 10^{-3}$, corresponding to a Reynolds number $Re = 1000$. Sutherland's law for viscosity has been used in the computations.

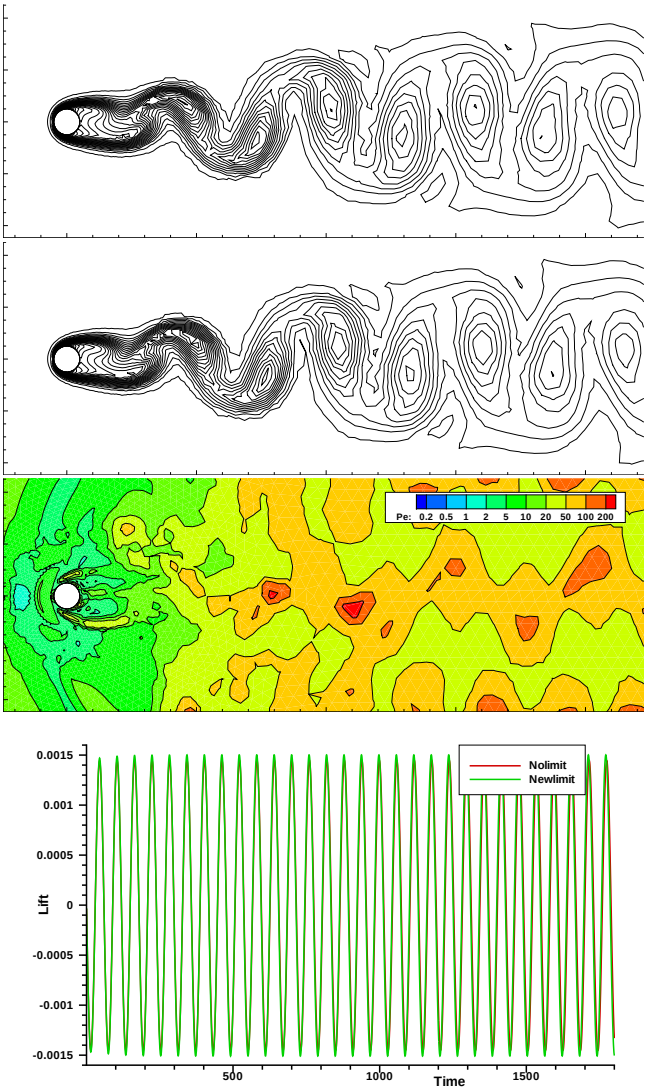

Figure 18: Top to bottom: Isolines of entropy, LDA scheme, standard approach. Isolines of entropy, LDA scheme, presented approach. Isolines of Peclet number. Lift dependence on time.

The speed of sound (and hence the density) in the initial solution is determined from the assumption of constant stagnation enthalpy

$$a^2 = a_1^2 + \frac{\gamma - 1}{2}(u_1^2 - u) \tag{67}$$

and $Ma_\infty = 0.8$. Constant initial static pressure $p = 1$ is assumed across the whole flow-field. The grid used consists of an isotropic triangulation stretched in the y-direction using the mapping

$$y = \frac{L_y}{2}\frac{\sinh(b_y\eta)}{\sinh(b_y)}, \tag{68}$$

where $\eta \in (-1, 1)$ and $b_y = 3.4$. The mesh contains 201×201 nodes. The computation has been run with the B scheme.

The solution at time $t = 160$ is shown in Fig. 19, where we plot 30 levels of isolines of the temperature. Comparing with the fourth order results of [19], our method shows all features of flow-field. There is very little difference between the numerical methods. The map of the cell Peclet number is also included.

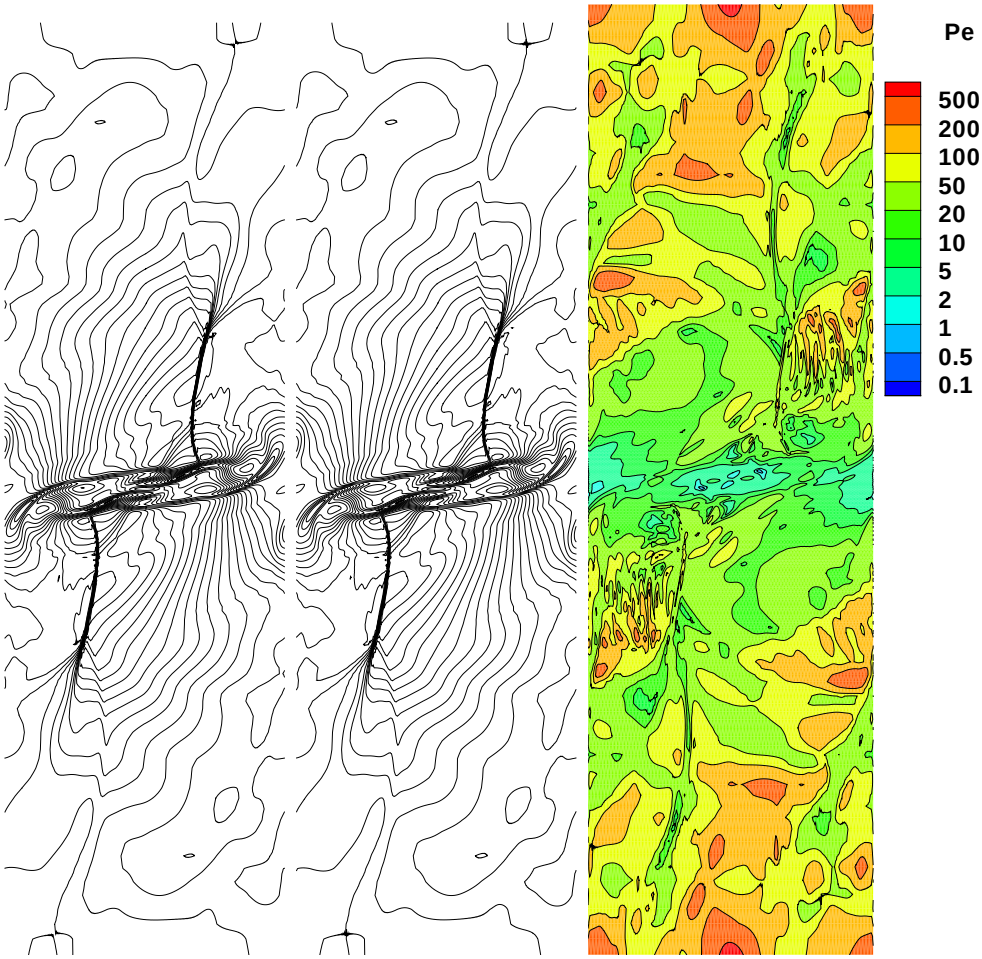

Figure 19: Transonic vortex pairing, mesh 201×201. Solution at $t = 160$. Bx scheme (see [7]). Left to right: Isolines of temperature – standard scheme, new approach. Isolines of Peclet number.

6 Conclusions

We have extended the approach of [12] for unsteady problems and system of Navier-Stokes equations. We have shown on numerically for scalar problem that the second order of accuracy is obtained, while with the previous attempt of [16, 10] gives only first order accurate schemes. However, we have also theoretically shown, that for problems of cell Peclet number larger than approx. 7.5, the previous approach is qualitativelly similar to the new hybrid approach. In this case, the hybrid approach does not bring any advantage and it is enough to use the standard scheme of [16, 10].

References

[1] T. J. Barth and D. C. Jesperson. The design and application of upwind schemes on unstructured meshes. AIAA Paper 89–0366, AIAA, Jan 1989.

[2] F. Bassi and S. Rebay. A high-order accurate discontinous finite element method for the numerical solution of the compressible navier-stokes equations. *Journal of Computational Phydics*, 131:267–279, 1997.

[3] Jiří Dobeš. Implicit space-time method for laminar viscous flow. Project Report 2002-06, Von Karman Institute for Fluid Dynamics, Belgium, June 2002.

[4] Jiří Dobeš, Mario Ricchiuto, and Herman Deconinck. Implicit space-time residual distribution method for unsteady laminar viscous flow. *33rd Computational Fluid Dynamics Course, Von Karman Institute for Fluid Dynamics*, 2003.

[5] Jiří Dobeš, Mario Ricchiuto, and Herman Deconinck. Implicit space-time residual distribution method for unsteady viscous flow. In *16th AIAA Computational Fluid Dynamics Conference, Orlando, Florida*, AIAA-2003-3691, 2003.

[6] Jiří Dobeš, Mario Ricchiuto, and Herman Deconinck. Implicit space-time residual distribution method for unsteady laminar viscous flow. *Computers and Fluids*, 34:593–615, 2005. ISSN 0045-7930.

[7] Jiří Dobeš and Herman Deconinck. Second order blended multidimensional residual distribution scheme for steady and unsteady computations. *Journal of Computational and Applied Mathematics (JCAM)*, 2005. Accepted for publication. Special issue of Third international conference on advanced computational methods in engineering ACOMEN 2005, Ghent, Belgium, May 30 – June 2, 2005.

[8] Antonino Ferrante and Herman Deconinck. Solution of the unsteady Euler equations using residual distribution and flux corrected transport. Project Report VKI PR 1997-08, Von Karman Institute for Fluid Dynamics, Belgium, June 1997.

[9] H. Nishikawa and P. Roe. On high-order fluctuation splitting schemes for Navier-Stokes equations. In *ICCFD 3. 3rd Interational Conference on Computational Fluid Dynamics*. Springer-Verlag, 2004.

[10] Henri Paillère. *Multidimensional Upwind Residual Distribution Schemes for the Euler and Navier-Stokes Equations on Unstructured Grids*. PhD thesis, Université Libre de Bruxelles, Von Karman Institute for Fluid Dynamics, June 1995.

[11] M. Ricchiuto, N. Villedieu, R. Abgrall, and H. Deconinck. High order residual distribution schemes: Discontinuity capturing crosswind dissipation and extension to advection–diffusion. CFD – High Discretization Methods. VKI Lecture Series 2006–01, Von Karman Institute for Fluid Dynamics, Chausée do Waterloo 72, B-1640 Rhode Saint Genèse, Belgium, 2005.

[12] M. Ricchiuto, N. Villedieu, R. Abgrall, and H. Deconinck. On uniformly high-order accurate residual distribution schemes for advectiondiffusion. *Journal of Computational and Applied Mathematics*, 2007. In press ; doi:10.1016/j.cam.2006.03.059.

[13] P. L. Roe. Approximate Riemann solvers, parameter vectors, and difference schemes. *J. Comput. Phys.*, 43:357–372, 1981.

[14] Hermann Schlichting. *Boundary-Layer Theory*. Mc-Graw-Hill, seventh edition edition, 1979.

[15] Kurt Sermeus and Herman Deconinck. Drag prediction validation of a multi-dimensional upwind solver. CFD-based aircraft drag prediction and reduction, VKI Lecture Series 2003–02, Von Karman Institute for Fluid Dynamics, Chausée do Waterloo 72, B-1640 Rhode Saint Genèse, Belgium, 2003.

[16] Edwin T. A. van der Weide. *Compressible Flow Simulation on Unstructured Grids Using Multi-dimensional Upwind Schemes*. PhD thesis, Technische Universiteit Delft, Von Karman Institute for Fluid Dynamics, 1998.

[17] R. Warming and Hyett. The modified equation approach to the stability and accuracy analysis of finite-difference methods. *Journal of Copmutational Physics*, (14):159–179, 1974.

[18] Frank M. White. *Viscous Fluid Flow*. McGraw-Hill Science/Engineering/Math, 1991.

[19] H. C. Yee, N. D. Sandham, and M. J. Djomehri. Low-dissipative high-order shock-capturing methods using characteriscic-based filters. *Journal of Computational Physics*, 150:199–238, 1999.

Centre de recherche INRIA Bordeaux – Sud Ouest
Domaine Universitaire - 351, cours de la Libération - 33405 Talence Cedex (France)

Centre de recherche INRIA Grenoble – Rhône-Alpes : 655, avenue de l'Europe - 38334 Montbonnot Saint-Ismier
Centre de recherche INRIA Lille – Nord Europe : Parc Scientifique de la Haute Borne - 40, avenue Halley - 59650 Villeneuve d'Ascq
Centre de recherche INRIA Nancy – Grand Est : LORIA, Technopôle de Nancy-Brabois - Campus scientifique
615, rue du Jardin Botanique - BP 101 - 54602 Villers-lès-Nancy Cedex
Centre de recherche INRIA Paris – Rocquencourt : Domaine de Voluceau - Rocquencourt - BP 105 - 78153 Le Chesnay Cedex
Centre de recherche INRIA Rennes – Bretagne Atlantique : IRISA, Campus universitaire de Beaulieu - 35042 Rennes Cedex
Centre de recherche INRIA Saclay – Île-de-France : Parc Orsay Université - ZAC des Vignes : 4, rue Jacques Monod - 91893 Orsay Cedex
Centre de recherche INRIA Sophia Antipolis – Méditerranée : 2004, route des Lucioles - BP 93 - 06902 Sophia Antipolis Cedex

Éditeur
INRIA - Domaine de Voluceau - Rocquencourt, BP 105 - 78153 Le Chesnay Cedex (France)
http://www.inria.fr
ISSN 0249-6399